Pressure drop in the combustor due to heat release. The analysis of the ideal rocket motor is based on the postulate that combustion takes place at constant pressure. In practice, the release of heat in the gas stream in the combustor is accompanied by a decrease of both static and stagnation pressures. The decrease is dependent on the Mach number at the hot end of the combustion chamber, and becomes larger as the ratio of combustor cross-sectional area A_c to throat area A_{th} approaches unity. The loss in stagnation pressure represents an undesirable increase in entropy, a decrease in the effective pressure ratio for expansion, and hence a loss in specific impulse. The following analysis deals with these effects.

As before, the subscripts i, c, th, and e refer to states at the injector end of the combustor, the hot end of the combustor, the nozzle throat, and the nozzle exit. Except for the nonzero velocity in the combustor, the conditions of the analysis are the same as for the ideal rocket motor.

Since the expansion in the nozzle is isentropic (heat release completed in the chamber) the Mach number at c is obtainable from Eq. 2-10:

$$\frac{A_c}{A_{th}} = \frac{1}{M_c}\left(\frac{1 + \frac{\gamma - 1}{2} M_c^2}{\frac{\gamma + 1}{2}}\right)^{\frac{\gamma+1}{2(\gamma-1)}} \tag{3-14}$$

The integrated momentum equation, for frictionless flow in a constant area duct, provides an expression for the decrease in static pressure in the chamber. It is assumed that $M_i \cong 0$.

$$p_i = p_c(1 + \gamma M_c^2) \tag{3-15}$$

The simplest way to treat the performance for the case of nonzero M_c is first to calculate the equivalent plenum chamber pressure and temperature corresponding to the conditions at c, and then to calculate the flow properties in the nozzle on the assumption that the gas flow originates from this plenum chamber. The temperature T_c^0 and pressure p_c^0 of the equivalent plenum chamber are really the stagnation temperature and pressure at station c. (See III,A for discussion of stagnation quantities.)

$$p_c^0 = p_c\left(1 + \frac{\gamma - 1}{2} M_c^2\right)^{\frac{\gamma}{\gamma-1}} \tag{3-16}$$

$$T_c^0 = T_c\left(1 + \frac{\gamma - 1}{2} M_c^2\right) \tag{3-17}$$

$$\Delta h_c = c_p(T_c^0 - T_i) \tag{3-18}$$

Eq. 3-18 is simply a statement of the conservation of energy, with the kinetic energy term $\frac{1}{2}V_e^2$ absorbed in the stagnation enthalpy $c_pT_c^0$.

Therefore, T_c^0 is the same as T_c in the ideal rocket motor of Eq. 2-7, that is, the so-called adiabatic flame temperature, or simply the chamber temperature. The static temperature T_c is less than the adiabatic flame temperature, by as much as 10 or 15 per cent for a throatless motor, but this is of no consequence for the exhaust velocity. Only the stagnation temperature matters, and this depends only on the thermochemical heat of reaction Δh_c.

Fig. G,3d compares the conditions of the equivalent plenum chamber with those of the actual chamber by presenting the ratios p_c/p_i, p_c^0/p_i,

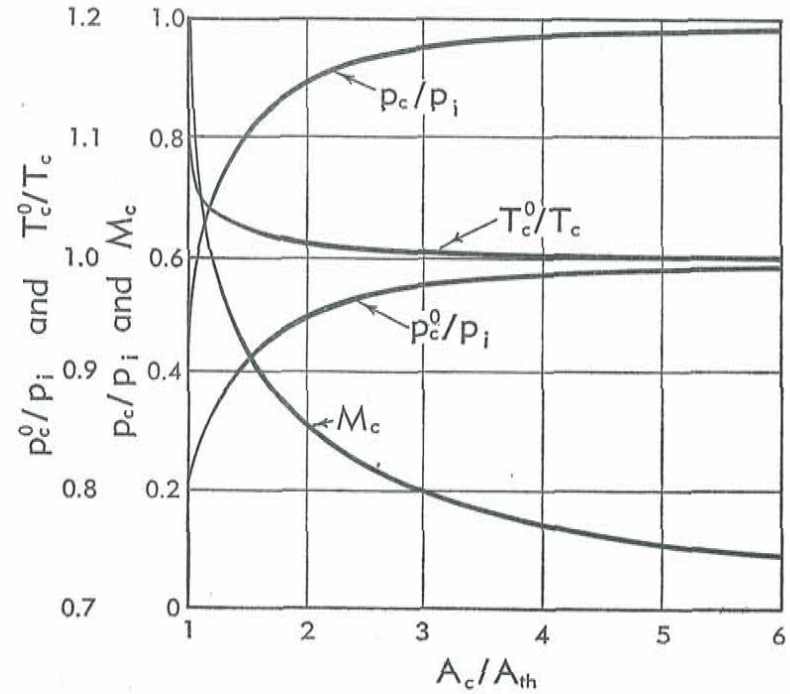

Fig. G,3d. Comparison of conditions in equivalent plenum chamber with those in actual combustion chamber.

M_c, and T_c/T_c^0 as functions of A_c/A_{th}. This figure is useful as a guide in carrying out the following computational procedure recommended for the performance analysis of a rocket motor.

In general, the particular propellant combination, the feed pressure, the nozzle throat area, the external pressure, and the chamber dimensions are specified in advance. The problem is to compute the effective exhaust velocity c, taking into account the effect of the pressure drop in the combustion chamber.

1. From the specified A_c/A_{th} and γ, compute M_c from Eq. 3-14.
2. With this M_c and the specified p_i, calculate p_c and then p_c^0 from Eq. 3-15 and 3-16.
3. From the specified ϵ of the nozzle, and the effective pressure ratio

p_c^0/p_∞, determine C_F^0 for the equivalent plenum chamber, from Fig. G,2d and G,2e.

4. The thrust is then calculated as follows:

$$F = C_F^0 p_c^0 A_{\text{th}} \tag{3-19}$$

5. The characteristic velocity c^* depends on the stagnation temperature, which is exactly equal to the adiabatic flame temperature. Therefore, $(c^*)^0$ is known, either by thermochemical calculation or by experiments with plenum-type combustors.
6. The mass flow is then calculated in terms of $(c^*)^0$:

$$\dot{m} = \frac{p_c^0 A_{\text{th}}}{(c^*)^0} \tag{3-20}$$

7. Finally, the effective exhaust velocity is calculated:

$$c = C_F^0 (c^*)^0 \tag{3-21}$$

In rocket testing, the chamber pressure is frequently measured at the forward end of the chamber, through a pressure tap drilled into the injector face. Clearly, this is p_i and not p_c^0. Unless the measured p_i is converted by Eq. 3-15 and 3-16 to p_c^0, the reported value of c^* will be too high by as much as 25 per cent (Fig. G,3b) for a throatless motor, and the reported value of C_F (experimental)/C_F (theoretical) will be low by a comparable error. These effects are significant for a rocket motor with a throat diameter equal to $\frac{1}{2}$ or more of the chamber diameter. If the combustor is not cylindrical, the preceding analysis must be modified. In particular, Eq. 3-15 holds only for cylindrical combustors; for other shapes, it is necessary to know the axial distribution of the heat release in order to integrate the momentum equation.

It may be noted that the same theory can be used to determine the axial distribution of heat release, i.e. the over-all kinetics of combustion. Thus, in a cylindrical chamber, the variation of M with axial position x is obtainable from the pressure distribution by means of Eq. 3-15. Then, from the equation of continuity (Eq. 3-22), the point-by-point static temperature can be computed, and from this, the stagnation temperature and the heat release.

$$\dot{m} = \frac{p A_c \mathfrak{M}}{[RT/\gamma M]^{\frac{1}{2}}} \tag{3-22}$$

G,4. Theoretical Specific Impulse Calculations. The calculation of specific impulse in the theory of the ideal rocket motor in Art. 2 is deficient in two very important respects: the combustion gas mixture is chemically reactive, and the specific heats vary strongly with temperature. Both these factors were ignored there. It is the purpose of this article to develop the complete theory, with both effects present. Inaswith respect to its operating parameters. The most important of these is the combustion pressure—the higher the pressure, the lower the propellant consumption rate for a given thrust; but at the same time, the greater the weight of the pressurization system. For the compressed gas type, the optimum pressure usually works out to lie between 250 and 400 lb/in.^{2}; for the turbopump system, the optimum is usually near 1000 lb/in.^{2}, but a lower pressure is always employed to ease the cooling problem. It is clear that the turbopump type is the most suitable one for long range, large size rockets with long firing durations.

2. Simplicity and ruggedness: The great simplicity of the compressed gas type makes it the most appropriate system for such applications as small anti-aircraft guided missiles, which have to be ready for instantaneous firing with high reliability with a minimum of prefiring inspection and adjustment. The same consideration applies to detachable JATO units.
3. Low cost: The consideration of cost is important mainly for civilian applications such as the take-off of heavy cargo planes, and perhaps rocket travel in the future. For military purposes, cost is significant mainly as an indication of manufacturing difficulty, and, therefore, for missiles or JATOs required in very large numbers, the gas-pressurized type is preferred.

G,8. Bibliography.

Article 1.

Dictionary of guided missile terms. Compiled by Ordnance Dept., U.S. Army. *Anti-Aircraft J.*, 1949.

Glossary of guided missile terms. Prepared by *Committee on Guided Missiles, Research and Develop. Board, U.S. Dept. of Defense, GM 51/3 and GM 51/8,* Sept. 1948.

Layton, J. P., and Youngquist, R. Proposed A.S.A. letter symbols for rocket propulsion. *Jet Propulsion 25*, 634 (1955).

Article 2.

Malina, F. J. Characteristics of the rocket motor unit based on the theory of perfect gases. *J. Franklin Inst. 230*, 433 (1940).

Seifert, H. S., and Crum, J. Thrust coefficient and expansion ratio tables. *Ramo-Wooldridge Corp.*, Feb. 1956.

Seifert, H. S., Mills, M. M., and Summerfield, M. The physics of rockets, Part I. *Am. J. Phys. 15*, 1 (1947).

Shapiro, A. H. *Dynamics and Thermodynamics of Compressible Fluid Flow*, Vol. I, Chap. 4. Ronald Press, 1953.

Sutton, G. P. *Rocket Propulsion Elements*, 2nd ed., Chap. 3. Wiley, 1956.

Article 3.

Banerian, G. Rocket performance with heat added to inlet propellants by regenerative and external means. *Jet Propul. 25*, 712 (1955).

Beckwith, I. E., and Moore, J. A. An accurate and rapid method for the design of supersonic nozzles. *NACA Tech. Note 3322*, Feb. 1955.

Dillon, P., and Line, L. E., Jr. Heat transfer between solid particles and gas in a rocket nozzle. *Jet Propul. 26*, 1091 (1956).

Durham, F. P. Thrust characteristics of underexpanded nozzles. *Jet Propul. 25*, 696 (1955).

Gilbert, M., Davis, L., and Altman, D. Velocity lag of particles in linearly accelerated combustion gases. *J. Am. Rocket Soc. 25*, 26–30 (1955).

Glassman, I. Impulse expressions for rocket systems containing a solid phase. *Jet Propul. 27*, 542 (1957).

Kogan, A. Boundary layer correction in supersonic nozzle scaling. *J. Aeronaut. Sci. 25*, 64 (1958).

Puckett, A. E. Supersonic nozzle design. *J. Applied Mech. 13*, A265-A270 (1946).

Seifert, H. S., and Altman, D. A comparison of adiabatic and isothermal expansion processes in rocket nozzles. *J. Am. Rocket Soc. 22*, 159–162 (1952).

Shapiro, A. H. *The Dynamics and Thermodynamics of Compressible Fluid Flow*, Vol. I, Chap. 7 and 15. Ronald Press, 1953.

Summerfield, M., Foster, C. R., and Swan, W. C. Flow separation in overexpanded supersonic exhaust nozzles. *Jet Propul. 24*, 319 (1954).

Sutton, G. P. *Rocket Propulsion Elements*, 2nd ed., Chap. 3. Wiley, 1956.

Article 4.

Battelle Memorial Inst. Physical properties and thermodynamic functions of fuels, oxidizers, and products of combustion. *Project Rand Repts. R-127, 129, 196*. Columbus, Ohio, 1949.

Charts of theoretical performance of several rocket propellant combinations. *Rocketdyne, Div. North Amer. Aviation, Inc.*, 1956.

Donegan, A. J., and Farber, M. Solution of thermochemical propellant calculations on a high speed digital computer. *Jet Propul. 26*, 164–172 (1956).

Fickett, W., and Cowan, R. D. Values of thermodynamic functions to 12,000°K for several substances. *Los Alamos Sci. Lab. Rept. 1727*, Sept. 1954.

Hottel, H. C., Williams, G. C., and Satterfield, C. N. *Thermodynamic Charts for Combustion Processes*. Wiley, 1949.

Huff, V. N., and Calvert, C. S. Charts for computation of equilibrium composition of chemical reactions in the C-H-O-N system from 2000°K to 5000°K. *NACA Tech. Note 1653*, July 1948.

Huff, V. N., and Gordon, S. Tables of thermodynamic functions for analysis of aircraft propulsion systems. *NACA Tech. Note 2161*, Aug. 1950. (Includes light metals and halogens, as well as C, H, O, and N compounds.)

Huff, V. N., and Morrell, V. E. General method for computation of equilibrium composition and temperature of chemical reactions. *NACA Tech. Note 2113*, June 1950.

Krieger, F. J. Chemical kinetics and rocket nozzle design. *J. Am. Rocket Soc. 21*, 179–185 (1951).

Lewis, B., and von Elbe, G. *Combustion, Flames and Explosions of Gases*, Chap. 13. Academic Press, 1951.

Natl. Bur. Standards. Selected values of properties of hydrocarbons. *Circular 461*, Gov't. Printing Office, 1947.

Natl. Bur. Standards. Tables of selected values of chemical thermodynamic properties, 3 vol. *Circular 500*, Gov't. Printing Office, 1952.

Penner, S. S. Thermodynamics and chemical kinetics of one-dimensional nonviscous flow through a Laval nozzle. *J. Chem. Phys. 19*, July 1951.

Pocket Data Book for Rocket Engines. Bell Aircraft Corp., Buffalo, N.Y., 1954. (Properties of fuels, oxidizers, and propellant combinations.)

Sutton, G. P., *Rocket Propulsion Elements*, 2nd ed., Chap. 4. Wiley, 1956.

Vichnievsky, R., Sale, B., and Marcadet, J. Combustion temperatures and gas composition. *J. Am. Rocket Soc. 25*, 105 (1955).

Article 5.

Baker, D. I. Mixture ratio and temperature survey of ammonia-oxygen rocket motor combustion chambers. *Jet Propul. 25*, 217 (1955).

Additional Material on Nozzle Flow Separation:

Performance Analysis of the Ideal Rocket Motor, Section G,3, Page 458, Equation (3-5); gives the nozzle static pressure (wall pressure) for flow separation for severely overexpanded conical nozzles as a function of atmospheric pressure, for determining the flow separation point for severely overexpanded conical nozzles.

The additional material which follows from NASA SP-8120, Liquid Rocket Engine Nozzles, provides the equivalent information for bell nozzles; the nozzle static pressure (wall pressure) for flow separation for severely overexpanded bell nozzles (contoured nozzles, parabolic contour nozzles) as a function of atmospheric pressure and chamber pressure, for determining the flow separation point for severely overexpanded bell nozzles.

From NASA SP-8120, Liquid Rocket Engine Nozzles:

2.1.2.1.3 Overexpanded Nozzle

Nozzles designed for vacuum operation have large expansion area ratios in order to achieve high specific impulse. It is desirable to ground test engines in the course of the development program. During ground testing, most altitude engines are overexpanded, often to the extent that the exhaust gas separates from the nozzle wall. This flow separation can result in serious problems. For example, a nonoptimum (parabolic) contour was selected for the nozzle of the J-2 engine in order to raise the exit wall pressure. The high-exit-pressure nozzle was supposed to run unseparated at an area ratio of 27 with a chamber pressure of 700 psi. A wall-pressure minimum that occurred between area ratio of 14 and the nozzle exit produced an unstable condition that caused unsteady asymmetric separation, especially during the startup. The large loads that occurred caused various thrust-chamber structural failures. A short bolt-on diffuser was developed to eliminate separation during mainstage operation of the J-2 (ref. 23). Restraining arms were attached from the test stand to the nozzle skirt to absorb the separation loads at startup.

Separation of flow occurs when the gas in the boundary layer is unable to negotiate the rise to ambient pressure at the end of the nozzle. The exact atmospheric pressure at which flow will separate from the wall of a nozzle cannot be predicted accurately. Various rules of thumb to predict separation have been suggested; however, general agreement on one of these methods has not been reached. An early rule stated that a danger of separation existed when the ratio of exit pressure to ambient pressure was equal to 0.4. Later methods based on fitting of experimental results accounted for the increase in overexpansion that can be obtained with increasing Mach number. A fit of experimental data for short contoured nozzles over a broad range of nozzle area ratios (ref. 24) indicates that separation will occur when

$$P_{wall}/P_{amb} = 0.583\,(P_{amb}/P_c)^{0.195}$$

where

P_{wall} = exhaust-gas static pressure on the wall at separation

P_{amb} = ambient pressure

P_c = chamber pressure = exhaust-gas total pressure

The method of reference 25 was the basis for a separation-prediction criterion that includes the effects of gas properties and nozzle shape on separation. A recent and fairly complete treatment of flow separation in nozzles is presented in reference 26. The results of the various prediction methods have shown agreement with experimental data in many cases, but in general predictions are used only as a guide.

NASA SP-8120 Overexpanded Nozzle References:

23. Anon.: J-2 Bimonthly Progress Report, November-December 1965. R-6300-3, Rocketdyne Div., North American Aviation, Inc., January 1966.

24. Schilling, M. T.: Flow Separation in a Rocket Nozzle. M. S. Thesis, University of Buffalo, June 1962.

25. Crocco, L.; and Probstein, R.: The Peak Pressure Rise Across an Oblique Shock Emerging from a Turbulent Boundary Layer Over a Plane Surface. Princeton University (Princeton, NJ), March 1964.

26. Schmucker, R. H.: Status of Flow Separation Prediction in Liquid Propellant Rocket Nozzles. NASA TM X-64890, November 1974.

HIGH POWER ROCKETRY JAN 1997

HIGH POWER
ROCKETRY

ASPIRING ROCKET SCIENTISTS GO TO SCHOOL

$4.95 CANADA $5.75 UK £4.95 01

0 74470 80373 7
JANUARY 1997

FEATURES

THE IDEAL ROCKET MOTOR

LAUNCH COVERAGE

MALINA'S WAC CORPORAL